Geological Quarterly, 2012, **56** (1): 25–40

The relationship of brine chemistry of the Pennsylvanian Paradox Evaporite Basin (southwestern USA) to secular variation in seawater chemistry

Oleh Yosypovych PETRYCHENKO, Sherilyn Coretta WILLIAMS-STROUD and Tadeusz Marek PERYT

Petrychenko O. Y., Williams-Stroud S. C. and Peryt T. M. (2012) – The relationship of brine chemistry of the Pennsylvanian Paradox Evaporite Basin (southwestern USA) to secular variation in seawater chemistry. Geol. Quart., **56** (1): 25–40.

To establish the brine chemistry associated with the evaporites in the Pennsylvanian Paradox Basin of southeastern Utah and southwestern Colorado (USA), the composition of presumably primary fluid inclusions was determined in sedimentary halite from two drill cores, one near the central part of the basin (Shafer Dome 1) and one from a more marginal location of the basin (Gibson Dome 1). Chemical analysis of halite fluid inclusions was made on six samples from three different evaporite cycles of the Paradox Formation: cycle 10 in the Shafer Dome core and cycles 6 and 18 from the Gibson Dome core. Inclusions that range in size from 2 to 80 microns across were analysed using the Petrychenko (1973) method. Large inclusions (40 to 80 microns across) that were analysed contain one fluid phase with a carnallite or sylvite daughter crystal. Also reported in this study are fluid inclusion homogenisation temperatures for sylvite or carnallite from primary or recrystallised halite crystals in the Gibson Dome 1, Shafer Dome 1, Cane Creek 1 and Elk Ridge 1 cores. The relationship between K^+ and Mg^{2+} in chloride-rich inclusions corresponds to their proportion in $MgSO_4$ – depleted marine waters concentrated to the stage of carnallite deposition. A correlative relationship was observed between K^+ and Mg^{2+} sulphate-rich inclusions and their predicted proportions in seawater not depleted in sulphate. In this suite of measurements, the sulphate-poor mineralogy and sulphate-poor inclusion brine compositions occur in the lower cycles of the Paradox Formation, while the sulhpate-rich mineralogy appears to be better developed in the shallower cycles. The mineralogy of the Paradox Basin Evaporite Formation has previously been explained by one of the authors (S. Williams-Stroud) as dues to the dolomitisation reaction of seawater brine with associated carbonates where mixing of seawater and meteoric water occurred in an evaporite basin that was intermittently closed to direct seawater inflow. However, the apparent temporal relationship of the mineralogy is also consistent with global seawater chemistry changes between $MgSO_4$-rich to $MgSO_4$-poor compositions that have been proposed by other workers. A transition from $MgSO_4$-rich to $MgSO_4$-poor seawater composition may have occurred between Pennsylvanian and Permian times. This paper presents a possible alternative explanation to those already proposed in the literature, that the Paradox Formation mineralogy resulted from an intermediate seawater composition that records the global transition from $MgSO_4$-rich to $MgSO_4$-poor seawater.

Oleh Y. Petrychenko, Institute of Geology and Geochemistry of Combustible Minerals, National Academy of Sciences of Ukraine, Naukova 3A, 79060 Lviv, Ukraine; Sherilyn Williams-Stroud, MicroSeismic, Inc., 1300 W Sam Houston Pkwy, Houston, TX, 77042, USA, e-mail: swmsstroud@microseismic.com; Tadeusz Marek Peryt, Polish Geological Institute – National Research Institute, Rakowiecka 4, 00-975 Warszawa, Poland, e-mail: tadeusz.peryt@pgi.gov.pl (received: April 7, 2011; accepted: Ocotober 10, 2011).

Key words: Paradox Basin, Pennsylvanian, evaporites, fluid inclusions, seawater chemistry.

INTRODUCTION

The existence of two chemical types of potash-bearing evaporite deposits has been widely recognized in the literature (Valiashko, 1962; Borchert and Muir, 1964; Hite, 1983; Hardie, 1984; Spencer and Hardie, 1990; Petrychenko *et al*., 2005). The mineralogy of potash evaporite deposits such as those in the Paradox Formation that are lacking or deficient in $MgSO_4$ minerals predicted to precipitate from modern seawater has been explained by sulfate depletion through brine mixing (Raup, 1970), dolomitisation of associated limestones (Williams-Stroud, 1994*a*), interaction with hydrothermal waters, and clay mineral cation exchange (Hardie, 1996). More recent work determining fluid inclusion compositions in primary halite shows that their brine composition is consistent with global fluctuations in the major ion composition of seawater during the Phanerozoic (Kovalevich *et al*., 1998; Lowenstein *et al*., 2001). At least one change in evaporite basin brine chemistry characterized by the Na-K-Mg-Ca-Cl (sulphate-poor) chemical composition, characteristic of the early Paleozoic and Devonian, to a brine chemistry characterized by a

Na-K-Mg-SO_4-Cl (sulphate-rich) composition, typical for the Permian, is interpreted to have occurred during the Carboniferous (Kovalevich *et al*., 1998). The majority of evaporite deposits from the Carboniferous reached only the gypsum/anhydrite evaporative stage, with only a limited number of potash evaporite basins preserved in the geological record during that period (Zharkov, 1984). Because of this lack of Carboniferous potash deposits and the lack of data on the chemical composition of relict brines in inclusions in sedimentary halite, it is difficult to draw conclusions about the rate and the transition time of one chemical type of brine in evaporite basins into the other.

The presence of kainite, langbeinite, kieserite, and other sulphate-bearing evaporite minerals (Table 1) has been used by previous workers to conclude the occurrence of Na-K-Mg-SO_4-Cl composition brines during primary deposition (Borchert and Muir, 1964). Polyhalite can also be associated with such a mineral association (Holland, 1984), but according to the experimental data of d'Ans (1915) the polyhalite can nucleate due to interaction of gypsum and concentrated brines of the Na-K-Mg-Ca-Cl type. Because of this possible back-reaction origin of polyhalite, it can be regarded as an indicator of the brine chemistry type only if other sulphate minerals are also present.

The middle Pennsylvanian Paradox Formation of southwestern USA is the only evaporite deposit from the Carboniferous for which extensive chemical data are available. Out of more than thirty halite-bearing cycles, eighteen reach potash mineralisation. The magnesium sulphate minerals kieserite and polyhalite have been identified together in the potash zone of cycles 6, 13 and 18 (Hite, 1961; Peterson and Hite; 1969; Raup and Hite, 1996). The Paradox Evaporite mineral paragenesis suggests that a sulphate-rich brine composition similar to that of modern seawater was present in this Pennsylvanian basin, but our preliminary data on inclusions in sedimentary halite in several cycles of the rock salt suggest that the brine chemistry of at least the earlier evaporite cycles lies on the sulphate-poor side of the Ca-SO_4 chemical divide (Spencer and Hardie, 1990; Hardie, 1996; Kovalevich *et al*., 1998). Sulphate was measured in the inclusion brines in sedimentary halite of cycle 18, but the concentration was at the lowest detectable level of SO_4^{2-} that can be measured by the Petrychenko method, about 0.5 g/l (Petrychenko, 1973; Petrichenko, 1979; Petrychenko and Williams-Stroud, 1995). In addition to the presence of sulphate, these samples contain up to 30 g/l $CaCl_2$ indicating these brines initially had a higher concentration of calcium than is characteristic of $MgSO_4$-rich seawater evaporites.

Table 1

Sulphate-bearing evaporite minerals interpreted to indicate seawater brines

Kainite	$MgSO_4 \cdot KCl \cdot 3H_2O$
Langbeinite	$K_2SO_4 \cdot 2MgSO_4$
Kieserite	$MgSO_4 \cdot H_2O$
Polyhalite*	$2CaSO_4 \cdot MgSO_4 \cdot K_2SO_4 \cdot 2H_2O$

* – because polyhalite can nucleate by interaction of gypsum with concentrating brines it should be considered part of a primary mineral paragenesis only if other sulphate minerals are also present

Williams-Stroud (1994*a*) previously attributed the origin of the brines to closed-basin interactions of brines similar to modern seawater composition with limestones and clays, combined with the mixing of basin brines. The brine-mixing and water-rock interaction model of Williams-Stroud effectively explains the mineralogy of the Paradox Evaporite Formation, but the stratigraphic position of this formation relative to the strong evidence of temporal fluctuations of seawater composition during the Phanerozoic indicates that examination of an alternative hypothesis for the observed mineral assemblage should be considered. In addition, there is currently no geochemical data available for coeval evaporite deposits reported in the literature, which leaves the Paradox Formation as the only potential representative of seawater composition from mid Pennsylvanian times.

Because evaporite deposition involves both chemical and hydrological evolution, recognizing the dominant factors that have influenced the development of a particular mineral assemblage can be difficult (e.g., Hardie, 1984; Fanlo and Ayora, 1998). An examination of the relative Ca and SO_4 concentrations in many ancient evaporite deposits by Kovalevich *et al*. (1998) showed that the scale of compositional influence from factors other than global seawater composition could be secondary when compared to secular changes of chemical composition of basin brines. In this paper we present the results of chemical analysis of fluid inclusions in seven samples from two locations in the Paradox Basin, and stable isotope data and fluid inclusion homogenisation data from the same cycles from four locations within the basin, with the aim of establishing the chemical type of brines that existed during deposition of evaporites in the Paradox Basin.

GEOLOGICAL SETTING

The Paradox Basin is located in southeastern Utah and southwestern Colorado (Fig. 1) and contains extensive evaporite deposits of middle Pennsylvanian age. The basin, located in the Colorado Plateau province, is usually defined by the extent of Paradox Formation salt, which was deposited in an elongate asymmetrical trough bounded to the north-east by the Uncompahgre Uplift (Fig. 1; Wengerd, 1958). The uplift is interpreted to have been a positive feature of high to moderately high relief, with the asymmetrical deep portion adjacent to the Uncompahgre fault line that defines the north-east basin margin (Johnson *et al*., 1991). Seawater access into the basin is interpreted to have been through the moderate to low relief platforms to the south-east, west and north-west (Hite, 1970).

Episodic incursions of seawater into the rapidly subsiding basin alternated with evaporitic periods, which resulted in the deposition of a cyclic succession of salt beds (Fig. 2) separated by clastic interbeds (Raup and Hite, 1992). As glacio-eustatic sea levels fluctuated, a sequence of evaporites estimated to be between 1800 and 2500 m thick was deposited in the foreland part of the Paradox Basin (Hite, 1961; Trudgill, 2011). The evaporite deposits interfinger with coarse clastics in the

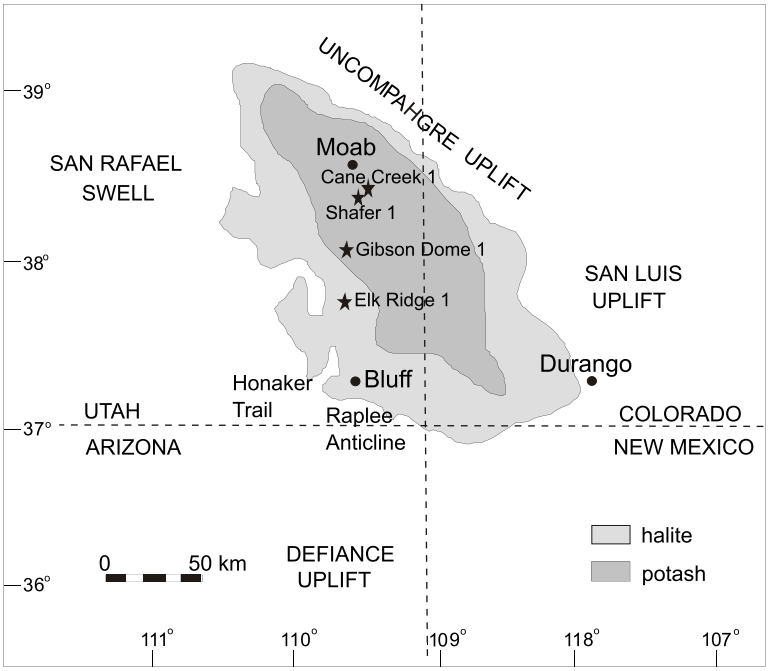

Fig. 1. Location of Shafer and Gibson Salt domes in the Paradox Basin (after Raup and Hite, 1996)

Dashed line oriented NE–SW through the basin indicates the approximate orientation of the schematic section in Figure 2; stars indicate core locations

foredeep on the eastern side of the basin and with carbonates around the basin margins. The Paradox Evaporite Formation itself consists of a cyclic deposit of a repetitive sequence of primarily halite, with minor clastics, organic shales and anhydrite, with economic oil and gas accumulations in some of the carbonates and black shales. Goldhammer *et al*. (1994) identified three superimposed orders of stratigraphic cyclicity in their study of the vertical stacking patterns of the marginal carbonate facies; each individual evaporite cycle is considered a fourth-order sequence (Weber *et al*., 1995). A total of thirty three halite-bearing cycles were identified by Hite (1961) in the Paradox Formation, numbered from cycle 29 at the base to cycle 1 at the top, with an additional four cycles above Hite's cycle 1 that were discovered by later drilling (Williams-Stroud, 1994*a*). Hite (1961) interpreted the base of each individual cycle to occur at beginning of a period of influx of seawater or a freshening of the brine, marked by an erosional or dissolutional contact between anhydrite and an underlying halite bed. The brine-freshening episodes represent the beginning of a period of influx of seawater, or a freshening of the brine in the basin due to sea level rise and climatic changes that resulted in increased precipitation (Hite and Buckner, 1981). The depositional environment during evaporite precipitation has been characterized as a restricted marine environment (Hite, 1970), and also as a playa salt deposit in a deep desiccated basin (Kendall, 1988). Evidence of both these end-member environments is present in the Paradox Basin (Williams-Stroud, 1994*a*). Each of the halite beds in the evaporite formation represent a depositional period of the order of only thousands of years, so that most of the Paradox Formation deposition could have occurred in either an open marine or restricted marine environment, as supported by the numerous carbonate shelf and algal mound deposits found within the basin (Hite and Buckner, 1981; Johnson *et al*., 1991; Goldhammer *et al*., 1994). Sub-aerial exposure evidence in the marginal facies such as chicken wire gypsum and halite dissolution features consistent with salt-pan halite deposition in some beds indicates that the environment in which the majority of the halite and gypsum evaporite deposition occurred may be characterized as a closed-basin, perennial saline lake, following the definition of Hardie *et al*. (1981).

Textures in the halite beds of the evaporite facies include euhedral cumulates with grain sizes of a few tenths of a millimetre, bottom growth halite crusts with crystal sizes up to 0.5 cm in diameter draped by fine-grained anhydrite, and mosaic fabrics found in the tops of the potash-bearing halite where the composition of the rock is more than 50% sylvite (Williams-Stroud, 1994*a*). Potash is found in eighteen of the halite cycles (Hite, 1985), and is present over a large area of the salt deposit (Fig. 1). The potash occurs as sylvite (KCl) or carnallite ($KMgCl_3 \cdot 6H_2O$) that generally occurs near the tops of the salt beds (Fig. 2). Salt beds in individual cycles have thicknesses of 7 to 270 m in the centre of the basin, pinching out to zero thickness on the flanks of the basin (Hite, 1961).

Identification of the depositional environments of evaporites is critical for any study of the brine chemistry that is done to determine the significance of the original brine composition, and several different environments of deposition are represented by the textures in the halite beds. The majority of the halite appears to have been deposited subaqueously, though there is also abundant evidence for sub-aerial exposure, particularly along the margins of the basin. Depositional textures indicating subaqueous exposure include the halite cumulates, which consist of small euhedral halite crystals formed by evaporation of brines near the surface which sink to the bottom of the brine pool and accumulate, and chevron halite crystals that grow up from the base of the brine pool (Williams-Stroud, 1994*a*). Though the halite cumulate is a primary depositional texture, it could form either as a result of brine mixing, or of high surface evaporation rates in a stratified brine (Kendall, 2011).

MATERIAL AND METHODS

Samples were analysed from a total of seven cycles from four different cores taken from the Paradox Basin (Fig. 1). The drill core locations include a location within the salt basin but outside the distribution of potash, Elk Ridge 1 (ER-1), a location within but near the boundary of the potash extent, Gibson Dome 1 (GD-1), and two locations that are near the centre of the basin, Shafer Dome 1 (SD-1) and Cane Creek 1 (CC-1). The CC-1 core location is the most basinal and is located where

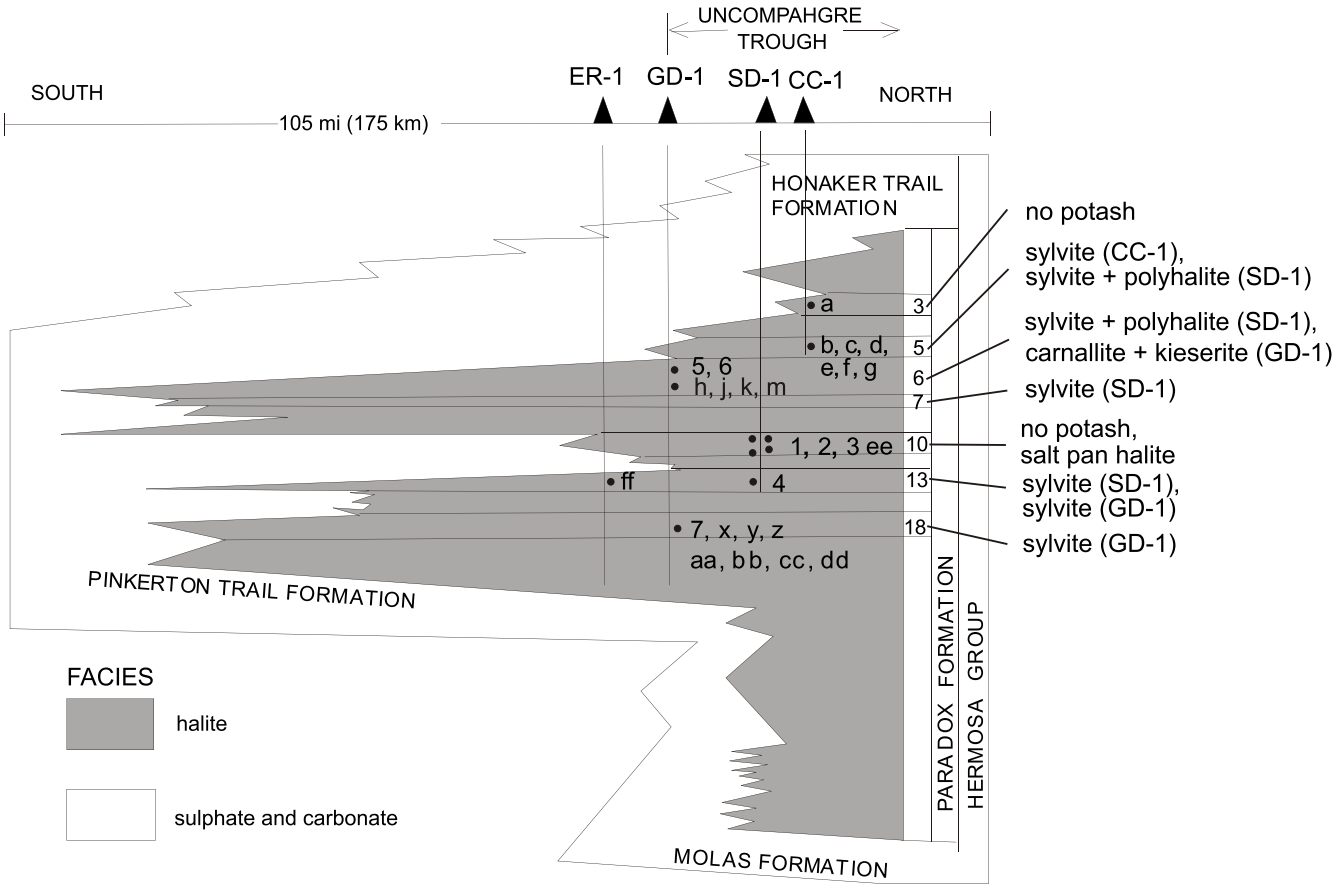

Fig. 2. Location of samples studied in the Cane Creek 1 (CC-1), Shafer Dome 1 (SD-1), Gibson Dome 1 (GD-1), and Elk Ridge 1 (ER-1) cores collected in the Paradox halite projected on the diagrammatic north-south cross-section across Paradox Basin, along the Utah–Colorado State line (after Raup and Hite, 1996)

Numbers and letters indicate samples listed in Table 2

the salt is thickest among the three core locations. Samples from cycle 6 were analysed from the SD-1 and GD-1, cycles 7, 10 and 13 from the SD-1, and cycles 3 and 5 from the CC-1 core, and cycle 13 was analysed from the ER-1 core. The only location from which the deepest cycle is this study, cycle 18, was analysed was the GD-1 core.

Three different types of analyses were performed on fluid inclusions in this set of studies:

1. Determination of the chemical composition of individual inclusions by the Petrychenko (1973) method;

2. Fluid inclusion homogenisation temperatures, which provide information about the temperature of brines during precipitation or recrystallisation and some qualitative information about salinity and relative amounts of solutes in the inclusion fluids;

3. Stable isotope analysis of inclusion brines.

The analyses include results that have been compiled from different studies done by the authors over the years, and although they lack a corresponding sample distribution (i.e. the sample locations and depths used to determine homogenisation temperatures is not the same as that used for the chemical analysis), there is enough overlap in the data sets to show trends in the chemistry of the halite. The fluid inclusion compositions were analysed using the Petrychenko (1973) method of glass capillaries with applied ultra-microanalytical techniques (see Lazar and Holland, 1988). This method makes it possible to select the most typical inclusions considering their size and phase composition (which usually is one-phase, fluid) and to eliminate the inclusions related to microfissures as well as the inclusions containing gas-oversaturated fluids. This is not the case when modern, high-precision analytical techniques of inclusion fluid extraction are applied (*cf.* Kovalevych and Vovnyuk, 2010).

The halite is dissolved with a thin jet of water to within a few tens of micrometers of the inclusion walls, and then, after the halite crystal is dried, the inclusion is opened. The inclusion fluid is extracted with a capillary tube (3 to 20 μm across), and a reagent is then added to determine the solutes in the inclusion fluid (see Petrychenko, 1979; Petrychenko and Peryt, 2004, for details). The capillary is then sealed and centrifuged. The volume of precipitate formed during this process is measured and then compared to that formed from a standard solution, accord-

ing to the formula published by Petrychenko (1973, see his table 4). Depending on the amount of the fluid extracted, all components or some of them can be studied in one inclusion; in the case of the sedimentary forms of the Paradox halite in >60% of inclusions studied all components have been determined. The analytical error of this method, after two to three repeated analyses, is 16–17% (Petrychenko, 1973). The minimum quantity of the studied ions needed for such an error is (in g/L): 0.8 for K, 1.0 for Mg, 0.9 for Ca, and 0.5 for sulphate ion, and the lower values are semi-quantitative. It is preferable to use average values of ion contents in inclusion brines of each sample for interpretations because the analytical error can be larger than possible changes of brine composition in different inclusions from the same sample.

Fluid inclusions in studied samples of sedimentary halite are arranged along the growth zones of the cubic crystals, occur in abundant accumulations and usually do not contain allogenic material. The inclusions are 2–80 μm across, usually 30–50 μm across. We have studied typical inclusions >40 μm across. It should be stressed that the typical size of inclusions in zoned halite crystals is important: there are known cases (e.g., middle Miocene – Badenian halite from Wieliczka, Southern Poland) of typical co-occurrence of large (up to >1 mm) and small (a few μm across) fluid inclusions that do not differ in composition, as established with the use of the Petrychenko (1973) method (Galamay *et al.*, 1997) and the cryo-SEM method (García-Veigas *et al.*, 1997).

Fluid inclusions in diagenetic halite are larger (>200 μm), isometric, can occur in groups or as separate forms without any regular pattern, often contain allogenic anhydrite and as a rule show a higher gas saturation.

Samples with two-phase inclusions containing daughter sylvite and/or carnallite crystals (typically 10–20 μm across) were chosen and heated to homogenise the inclusions. Heating runs were performed using a chamber with an accuracy of 0.5°C, and the heating rate was 0.5–1°C/min. In three halite samples, bromine content was determined by X-ray fluorescence (using a *Philips PW 2400* spectrometer): sample 1 – 80 ppm, sample 3 – 117 ppm, sample 5 – 195 ppm; these values fit well with the extensive set earlier published by Raup and Hite (1996).

Gas saturation was measured using the following procedure. The sample with fluid inclusions was heated for 6–8 hours at a temperature of 110–120°C which led to overheating of fluid inclusions and to the formation of microcracks around the individual inclusions and their filling by fluid. During the cooling of the sample to room temperature, the volume of solution was decreasing as, after cooling, part of it had a smaller volume compared to the original one. Such a deficit of solution volume was compensated by dissolved gases and water vapor. Subsequently, the slide was gradually dissolved in a 30–40%-water solution of glycerine that contained a CO_2 absorbant, i.e. $Ba(OH)_2$. The examination of the gas fraction was carried out under the microscope, in plane light. The diameter of the gas bubble was measured prior to and after the inclusion opening as well as after CO_2-reagent absorption, and then the gas pressure was calculated applying the Henry principle. For simplicity it was assumed that the average gas (nitrogen + methane) saturation in NaCl-saturated brines is 2 cm^3/l. The chemical composition of inclusions was also estimated by observing the freezing/melting behaviour of the fluid (Davis *et al.*, 1990). The temperatures for final melting of ice in the inclusion was recorded, and correlated with the presence of a daughter crystal of sylvite (for KCl concentration) or carnallite (for $MgCl_2$ concentration). These values were used as a rough indicator of the presence of magnesium chloride-rich *versus* potassium chloride-rich brines.

The measurements of homogenisation and dissolution temperatures were carried out on a petrographic microscope fitted with a fluid inclusion heating-cooling stage. The measurements of dissolution temperatures are taken as a more reliable indicator of temperature of crystallisation because of the possibility of vapor bubble origin by stretching of the inclusion after exposure to high temperatures (Roedder, 1984). Fluid inclusion daughter crystal dissolution temperatures were recorded and categorized by chevron halite textures, isolated inclusions, and fluid inclusion textures, whether they contained sylvite or carnallite daughter crystals, or no daughter crystal at room temperature.

Stable isotope analyses were done on samples from cycles 3 and 5 (CC-1 core), cycles 6 and 13 (GD-1 core), and cycles 6, 7 and 10 (SD-1 core). The values of $\delta^{18}O$ and δD were measured using an inductively coupled plasma mass spectrometer, and are interpreted as an indicator of source waters flowing into the basin by comparison to the isotope ratios in modern seawater and in modern meteoric water (Kyser, 1987).

DESCRIPTION OF SAMPLES

A total of 48 halite samples were selected from the four different cores taken through the Paradox Evaporite Formation. The locations of the cores (Fig. 1) shows that two of the cores (Cane Creek 1 and Shafer 1) are in a basinal location in the middle of the potash facies, the Gibson Dome 1 core is on the edge of the potash facies, and the one sample analysed from the Elk Ridge 1 core is within the halite facies but outside of the potash facies. The schematic cross-section of Figure 2 shows the relative locations of the core samples with the halite beds sampled from each core.

Sample 7, from cycle 18 in the GD-1 core, is the oldest halite cycle analysed in this study. Potash mineralisation is present in a thin interval near the top of cycle 18 in the form of sylvite and carnallite (Hite, 1961). Evaporites of cycle 18 were deposited after sedimentation of the thick evaporite sequence of cycle 19 where potash mineralisation occurs primarily in the form of sylvite (Hite, 1983). The bromine concentration is high at the very base of salt bed 18 (180 ppm) and quickly drops to about 80 ppm within a few feet above the base, indicating mixing of meteoric water with the highly concentrated brines of the underlying cycle (Hite, 1985). The halite analysed is laminated, with laminae 10 to 15 mm thick composed of relatively large (up to 10 mm across) crystals of bottom-growth halite. Fluid inclusions show a zonal pattern, and in some cases they outline almost the full form of the crystal cube. The inclusions contain brine and daughter crystals of sylvite or carnallite. The larger inclusions (>50 μm) contain carnallite and are interpreted to

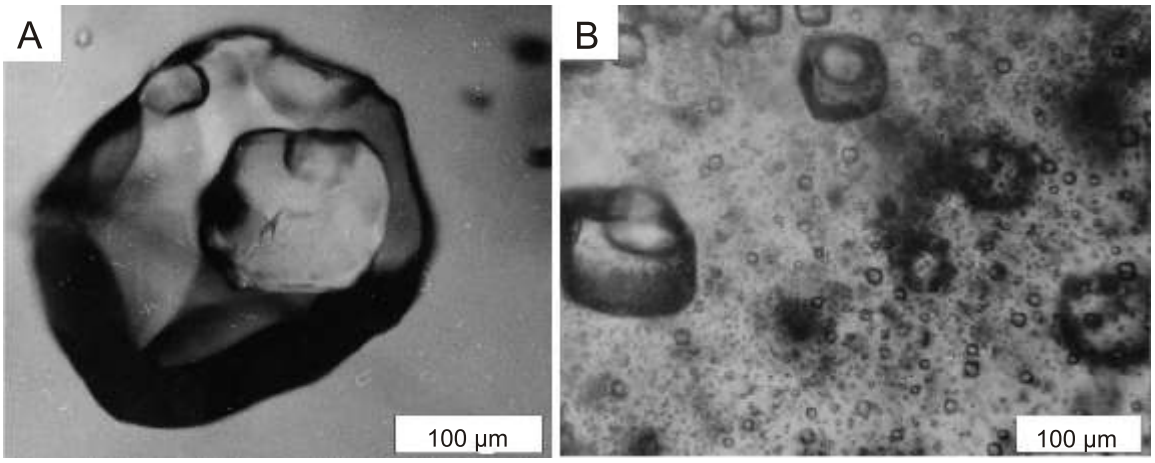

Fig. 3. Inclusions of salt-forming brines in halite from the Pennsylvanian Paradox Formation, Gibson Dome

A – fluid inclusion with a large carnallite daughter crystal in the zone of overgrowth of sedimentary by diagenetic halite (cycle 18, depth 1371.3 m, sample 7); **B** – inclusions in sedimentary halite with carnallite daughter crystal at the periphery and one-phase inclusions in the central part of the grain (cycle 6, depth 954.6 m, sample 5)

have formed in recrystallised halite (Fig. 3A), and smaller inclusions contain sylvite.

Sample 4 comes from cycle 13. Halite from near the base of salt bed 13 contains layers of fine-grained (1 mm grain size), relatively pure halite 2–5 cm thick, alternating with layers of coarser-grained (5 mm to 1 cm) euhedral halite with anhydrite. There is a weak vertical elongation of the coarser-grained halite crystals, which are rimmed by fine-grained anhydrite. Fluid inclusions in the larger crystals are isolated, and none contain sylvite crystals at room temperature. Near the top of salt bed 13 in the SD-1 core is a potash zone containing sylvite-rich layers with euhedral halite grains in a framework – supported fabric. The sylvite forms contiguous crystals in former void spaces. These layers alternate with layers of small cubic halite (0.1–0.2 mm) crystals rimmed by fine-grained anhydrite. Each halite crystal in this layer is defined by a core of rows of mutually perpendicular fluid inclusion banding. These layers of small cubic halite crystals (Fig. 4D) are probably a type of halite cumulate formed when evaporation of brine causes precipitation of small crystals on the brine-air interface (Lowenstein, 1982; Lowenstein and Spencer, 1990). When the crystals grow to a size (several mm) that could no longer be supported by the surface tension of the brine, they sink down to the bottom and pile up in the cumulate layer. Cumulate layers can also form as a result of brine mixing. Fine-grained halite cubes from 1 to 250 mm were precipitated experimentally by Raup (1970) from mixing of brines at the interface between brines of different compositions. The small grain size of the layers of halite cubes in the potash zone at the top of cycle 13 halite in the SD-1 core suggests the crystals more likely were formed as a result of a brine mixing mechanism.

The fluid inclusions that were analysed for brine composition (sample 4, SD-1 core, cycle 13) are composed of interbedded sylvite (1–2 cm thick) and halite of mixing-brine origin with finely crystalline anhydrite. In the mixing-brine halite, inclusions are one-phase fluid, zonal arranged, and <20 µm across (mostly <10 µm). Brine inclusions are characterized by a very high gas content – up to 70 cm^3/l. Individual crystals of mixing-brine halite reach 200 µm (Fig. 4A). Some of the larger euhedral halite crystals containing isotropic cubic inclusions do not respond to heating or cooling; these inclusions are probably solid sylvite crystals within the halite.

Samples 1–3 come from cycle 10. The halite of the cycle 10 is potash-barren. Salt bed 10 is distinctive in that internal layering in the salt from the SD-1 core is almost non-existent in portions of the core, but remnants of fluid inclusion-rich primary halite crystal growth are abundant. The crystal edges of the fluid inclusion-rich halite are rounded, and often occur in patches (1–8 mm across) where “chevron” and “cornet” crystals are found in coarsely crystalline clear diagenetic halite. Sedimentary halite contains clear fluid inclusions up to 80 µm across, with the majority of the inclusions <40 µm across. The secondary inclusions are gas-fluid and these can reach 800 µm across (Fig. 4C).

In sample 3 only diagenetic inclusions, >100 µm across, gas-fluid, occur; they contain xenogenic material (usually anhydrite – Fig. 4B). The inclusions that are <40 µm across are one-phase fluid. The diagenetic inclusions in this sample are as large as 500 µm across. Such large inclusions in samples 1–4 are very rare. The sedimentary texture of the samples 1–3 and the lack of daughter crystals in all of the inclusions analysed from cycle 10 suggest deposition of recycled halite in a salt pan environment; the small inclusions in these samples are not deposited from primary seawater brines.

Samples 5 and 6 come from 954.6 m in the rock salt of cycle 6 in the GD-1 core, which is overlain by potash deposits. The rock salt itself is composed of diagenetic halite with rare grains of sedimentary halite. Inclusions in the sedimentary halite are two-phase with sylvite or carnallite. The smaller, zoned inclusions contain sylvite daughter crystals, and the zones of clear halite that appeared to be void-filling precipitates generally contain a carnallite crystal when a daughter crystal is present. Within individual grains of sedimentary halite, centre inclusions are <40 µm with a sylvite daughter crystal or without a solid phase. Closer to the grain periphery, in-

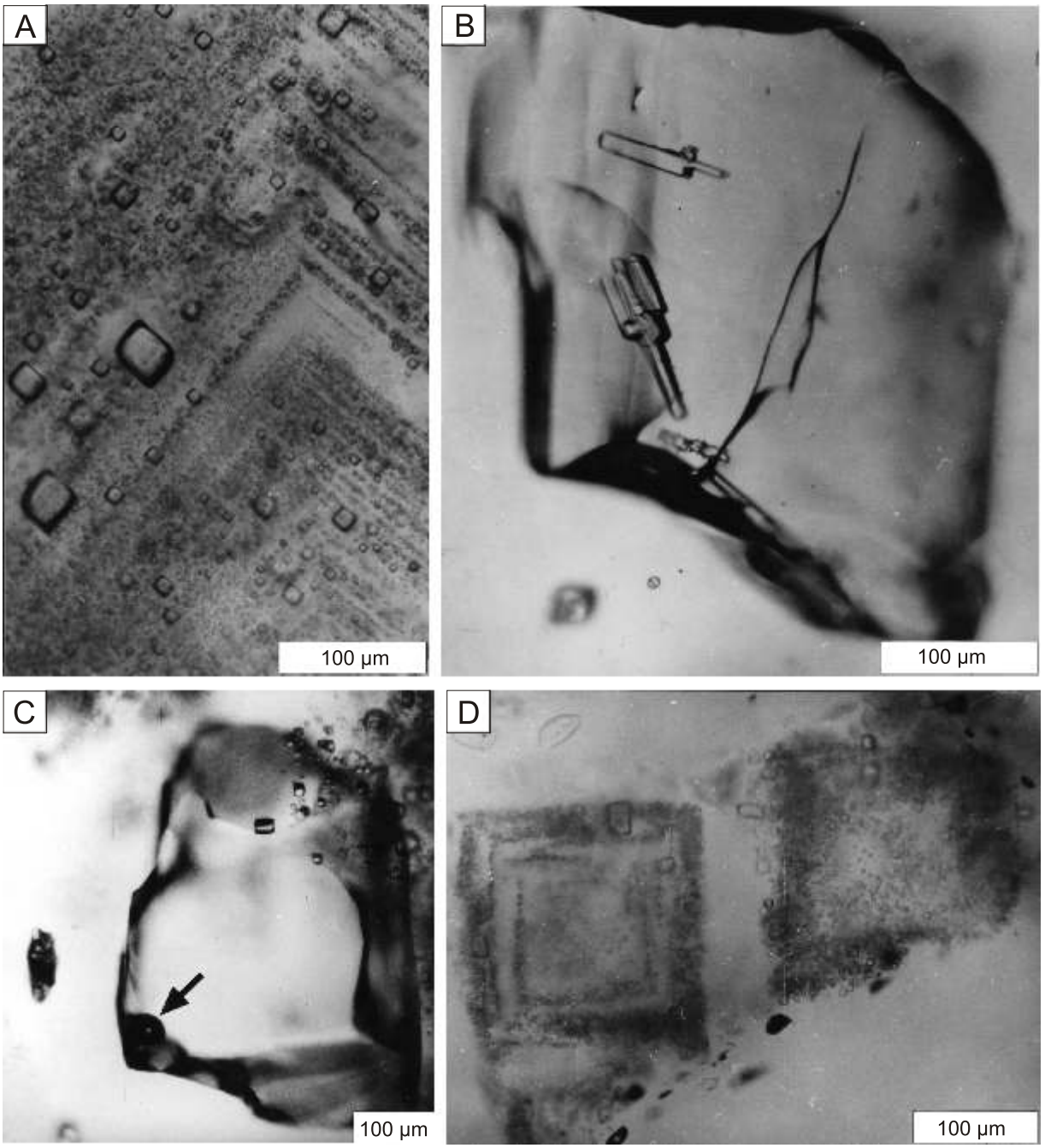

Fig. 4. Inclusions of salt-forming brines in halite from the Pennsylvanian Paradox Formation, Shafer Dome 1

A – one-phase inclusions in zoned sedimentary halite (cycle 13, depth 1215.5 m, sample 4); **B** – large fluid inclusion with anhydrite crystals in diagenetic halite (cycle 10, depth 1175.2 m, sample 3); **C** – inclusions with gas phase (arrowed) which originated at the periphery of sedimentary halite (cycle 10, depth 1134.9 m, sample 1); **D** – zoned halite crystal of brine-mixing origin with one-phase fluid inclusions (cycle 10, depth 1140.0 m, sample 4)

clusions are larger (up to 80 µm and even more) and contain a carnallite daughter crystal (Fig. 3B), possibly the result of entrapment of carnallite crystals precipitating via back-reaction of the brine with existing precipitates as halite cement formed around the sedimentary halite crystals.

RESULTS

The results are shown in Tables 2–4 and in Figures 5–7. Table 2 shows the fluid inclusion daughter crystal and gas phase homogenisation temperatures, ice melting temperature (C), gas content (cm^3/l) measured in the core samples. Hydrogen (deuterium) and oxygen stable isotope ratios were measured in the

Table 2

Homogenisation temperatures, fluid inclusion content, stable isotopes, and inclusion types analysed in halite cores from the Paradox Formation

Sample no.	Sample source	Depth [m]	Cycle	T_D [°C] daughter (carnallite)	T_D [°C] daughter (sylvite)	T_H [°C] gas phase	T_{MELT} [°C] ice	Gas content [cm^3/l]	$\delta^{18}O$ [‰]	δD [‰]	Inclusion content [at 26°C]	Inclusion type
a	CC-1	712.0	3			59	–36		3.6	–39	single phase	isolated
b	CC-1	821.1	5		33		–38				single phase	isolated
c	CC-1	832.7	5		106		–30		–1.7	–37	two-phase, w/daughter	fluid inc. banding
d	CC-1	826.0	5		85						two-phase, w/daughter	fluid inc. banding
e	CC-1	826.0	5		36						single phase	isolated
f	CC-1	837.3	5		70						two-phase, w/daughter	fluid inc. cluster
g	CC-1	850.4	5		60				–0.7	–52	single phase	isolated
h	ER-1	837.4	6			85	–27				single phase	isolated
ff	ER-1	958.8	13						–0.4	–72	single phase	chevrons
5	GD-1	954.6	6	99	78			3.0			two-phase, w/daughter	primary
	GD-1	954.6	6	97	76			4.0			two-phase, w/daughter	primary
	GD-1	954.6	6	108	82			3.0			two-phase, w/daughter	primary
6	GD-1	955.0	6								two-phase, w/daughter	primary
m	GD-1	954.3	6	93	78	30	–38					
n	GD-1	954.6	6	105	98	45			–7.7	–61	two-phase, w/daughter	chevron and isolated
o	GD-1	954.6	6		68	63						
p	GD-1	954.6	6		64	79	–17		–10.2	–82		
q	GD-1	987.5	6	109		50			–3.8	–70	two-phase, w/daughter	isolated, secondary
r	GD-1	997.3	6		108				–11.2	–101		isolated
s	GD-1	1021.4	6		46	49						isolated
7	GD-1	1371.2	18	82	87			40.0			two-phase, w/daughter	primary
	GD-1	1371.2	18	86	89			60.0			two-phase, w/daughter	primary
	GD-1	1371.2	18	84				50.0			two-phase, w/daughter	primary
t	SD-1	937.0	6		44						single phase	isolated
u	SD-1	963.5	6		35						two-phase, w/daughter	fluid inc. banding
v	SD-1	984.5	6		61		10					isolated
w	SD-1	995.5	6		57		–54				two-phase, w/daughter	isolated ?primary
x	SD-1	1017.9	7		29		–37					fluid inc. cluster
y	SD-1	1020.9	7		28		–35					sparse banding
z	SD-1	1024.6	7		38		–30					isolated
aa	SD-1	1027.5	7		36		–38					isolated
bb	SD-1	1027.5	7		43		–38					fluid inc. cluster
cc	SD-1	1030.8	7		48		–38		0.15	–56		isolated
dd	SD-1	1034.2	7		36		–34		1.8	–45		isolated
1	SD-1	1134.9	10			33		3.5			two-phase, gas bubble	primary, chevron
	SD-1	1134.9	10			31		1.5			two-phase, gas bubble	
	SD-1	1134.9	10			33		2.0			two-phase, gas bubble	

Tab. 2 cont.

Sample no.	Sample source	Depth [m]	Cycle	T_D [°C] daughter (carnallite)	T_D [°C] daughter (sylvite)	T_H [°C] gas phase	T_{MELT} [°C] ice	Gas content [cm^3/l]	$\delta^{18}O$ [‰]	δD [‰]	Inclusion content [at 26°C]	Inclusion type
2	SD-1	1140.0	10			29		3.0			one-phase	primary, chevron
	SD-1	1140.0	10			29		3.0			one-phase	
	SD-1	1140.0	10					1.8				
2	SD-1	1140.0	10									secondary
3	SD-1	1175.2	10								one-phase + trapped anhydrite	secondary, isolated
ee	SD-1	1141.0	10				–33		–9.6	–67	one-phase	chevrons
4	SD-1	1215.5	13			29		60.0				primary
gg	SD-1	1218.6	13		49						two phase, w/daughters	cummulate banding
hh	SD-1	1262.8	13		30		–44				two phase, w/daughters	isolated
jj	SD-1	1264.4	13			36	–45					
kk	SD-1	1257.1	13		34	60						isolated

Gray shaded cells denote samples analysed for chemical composition by the Petrychenko (1973) method; core sample sources: CC-1 – Cane Creek 1, ER-1 – Elk Ridge 1, GD-1 – Gibson Dome 1, SD-1 – Shafer Dome 1; T_D – decrepitation temperature; T_H – homogenization temperature; T_{MELT} – melting temperature

samples selected, and are also shown in Table 2. The description of the inclusion contents and types of inclusions (Table 2) and the sedimentary textures of the halite samples (Fig. 3) were used to classify the samples as either primary depositional sedimentary halite or diagenetic halite. The results of the chemical study of inclusion brines from sedimentary (primary) halite are shown in Table 3 and results from diagenetic halite are shown in Table 4. The locations of the samples which were analysed for their chemical composition are highlighted in the gray shaded cells in Table 2.

CYCLE 18

Homogenisation temperatures of inclusions with carnallite of cycle 18 are 82–86°C, and with sylvite are 87–89°C (Table 2). The brines of those inclusions are highly gas-saturated (40–60 cm^3/l). The chemical analyses of several inclusions from this sample show high concentrations of magnesium and calcium, with smaller potassium concentrations. The sulphate content is at the detection limit of the Petrychenko method (0.5 g/l). The results shown in Table 3 indicate a magnesium sulphate-poor brine. The data refer to the inclusion fluids from which carnallite has precipitated, and Figure 7 (point 7) shows the composition of the inclusion brine close to the carnallite-bischofite mineral stability fields. However, the results of analyses of inclusion brines with sylvite or carnallite crystals are not suitable for the reconstruction of chemical composition of ocean water (Zimmermann, 2000; Horita *et al.*, 2002), as the ratios of the principal ions in brines of such high concentration can substantially differ from ratios of seawater from which those brines have originated.

Stable isotope values for δD and $\delta^{18}O$ from a sample from cycle 10 at 1141 m (Table 2) are one of three sample results with values nearest to the meteoric water trend of all samples measured (Fig. 5). None of the inclusions measured in this cycle contained daughter crystals, and none were precipitated when the inclusions were cooled (Table 2).

CYCLE 13

The small sizes of fluid inclusions (<20 μm) in sample 4 shown in Figure 4D made it possible to realize only qualitative analyses for the presence of Ca and SO_4 ions; they revealed the presence of Ca ions and the SO_4 content was close to the detection limit (Table 3). Brine inclusions are characterized by a very high gas content – up to 70 cm^3/l (Table 2).

CYCLE 10

Chemical analyses of samples 1 and 2 showed a low gas content (1.5–3.5 cm^3/l) in fluid inclusions in sedimentary halite (Table 2). In transparent halite which we interpret to be of diagenetic origin, gas-fluid inclusions (Fig. 4C) containing 20 cm^3/l of gas were recorded. The homogenisation temperatures of those inclusions range from 29 to 33°C (Table 2). The fluid inclusions in sedimentary halite (Table 2) are of $CaCl_2$ type.

Fluid inclusions in diagenetic halite of samples 2 and 3 are shown in Table 4. The homogenisation temperature of those inclusions is 29°C (Table 2). Rare, very large fluid inclusions in diagenetic halite of sample 3 are of $CaCl_2$ type as well but they are characterized by much higher Ca concentration; the composition of brine inclusions in one such large inclusion (500 μm) is shown in Table 4.

Table 3

Chemical composition of inclusion brines in sedimentary (presumably primary) halite of the Paradox Formation

Sample no.	Sampling location			Content [g/l]				Indices			
	Well	Depth [m]	Cycle	K^+	Mg^{2+}	Ca^{2+}	SO_4^{2-}	2K	Mg	Ca	SO_4
1	SD-1	1134.9	10	11.0	54.8	5.7	0.5				
				14.5	56.2	7.7	0.5				
				15.3	53.7	8.3	0.5				
				n.d.	57.0	10.2	0.5				
				n.d.	n.d.	4.5	n.d.				
				13.6	**55.4**	**7.2**	**0.5**	**6.4**	**86.9**	**6.8**	
2	SD-1	1140.0	10	9.6	35.1	9.1	0.5				
				13.7	38.4	5.8	0.5				
				11.0	25.7	7.9	0.5				
				11.4	**33.0**	**7.6**	**0.5**	**8.7**	**80.2**	**11.1**	
4	SD-1	1215.5	13	n.d.	n.d.	traces	0.5				
5	GD-1	954.6	6	3.3	70.0	0.7	27.1				
				5.6	81.1	0.7	23.3				
				3.1	n.d.	n.d.	33.2				
				4.0	**75.5**	**0.7**	**27.8**	**1.4**	**90.2**		**8.4**
6	GD-1	955.0	6	5.5	90.0	0.7	36.1				
				7.8	78.8	0.7	23.2				
				7.7	83.8	n.d.	32.5				
				8.0	n.d.	n.d.	25.3				
				n.d.	n.d.	n.d.	24.7				
				7.2	**84.2**	**0.7**	**28.3**	**2.3**	**90.0**		**7.7**
7	GD-1	1371.2	18	6.9	57.8	49.4	0.5				
				7.6	59.3	59.4	0.5				
				10.7	50.4	57.7	0.5				
				8.8	n.d.	33.3	n.d.				
				n.d.	n.d.	n.d.	n.d.				
				8.4	**55.8**	**49.9**	**0.5**	**3.0**	**63.2**	**33.8**	

Average values are shown in bold; n.d. – not determined

Table 4

Chemical composition of inclusion brines in diagenetic halite

Sample no.	Depth [m]	Cycle	Content [g/l]				Indices		
			K^+	Mg^{2+}	Ca^{2+}	SO_4^{2-}	2K	Mg	Ca
2	1140.0	10	13.8	33.8	9.0	0.5			
			13.2	25.4	7.5	0.5			
			14.5	23.2	8.0	n.d.			
			n.d.	22.0	n.d.	n.d.			
			13.8	**26.1**	**8.1**	**0.5**	**12.2**	**74.1**	**13.7**
3	1175.2	10	17.7	39.9	44.4	0.5			
			21.0	50.0	28.8	n.d.			
			n.d.	n.d.	33.3	n.d.			
			tn.d.	n.d.	n.d.	n.d.			
			19.0	**44.9**	**35.5**	**0.5**	**8.3**	**62.1**	**29.6**

All samples are from Shafer Dome 1, cycle 10; for other explanations see Table 3

CYCLE 6

Inclusions in the sedimentary halite of samples 5 and 6 are two-phase with either a sylvite or carnallite daughter crystal. Within individual grains of sedimentary halite, centre inclusions are <40 μm with a sylvite daughter crystal or without a solid phase. Closer to the grain periphery, inclusions that appear to be in diagenetic halite possibly formed by dissolution and reprecipitation of the original primary crystal are larger (up to 80 and even 120 μm) and contain a carnallite daughter crystal (Fig. 3B). The homogenisation temperatures and gas contents are shown in Table 2. Brine inclusions in these samples have a relatively high content of sulphate (23–36 g/l; Table 3). The contents of Ca and Mg are in the range expected for brines from which carnallite has precipitated, and they are located close

to the boundary of stability fields of chloride minerals: carnallite and bischofite, and the sulphate mineral kainite (Fig. 7).

INTEPRETATION AND DISCUSSION

The results suggest the presence of two types of salt-forming brines: Ca-rich and sulphate-rich. An apparent trend of $MgSO_4$ enrichment can be seen from the lowermost beds sampled of the evaporite sequence to the youngest beds. The models of Kovalevich (1988) and Hardie (1996) both attribute changes in evaporite composition to changes in seawater chemistry. The Hardie model concentrates largely on fluctuations of the Mg/Ca ratio due primarily to hydrothermal brine flux from mid-ocean ridge spreading. Mg/Ca ratios larger than 2 are associated with aragonite seas from which high Mg calcite or aragonite precipitate, and Mg/Ca ratios less than 2 produced calcite seas (Hardie, 1996). Kovalevich (1988) proposed that secular variation in seawater was caused by volcanism and mid-ocean ridge spreading, changes in sea level, climate, atmospheric composition, and biosphere evolution. Variations in seawater composition in this model are dependent on the amount of SO_4 in the seawater system. Both Hardie (1996) and Kovalevich *et al.* (1998) identified trends in the evaporite sedimentary record that place the Pennsylvanian Paradox Formation in a transitional composition, intermediate between the $MgSO_4$-rich Permian evaporites and the $MgSO_4$-poor evaporite deposits of the Devonian. Petrychenko *et al.* (2002) showed that the Visean waters were characterized by Na-K-Mg-Ca-Cl-type brines, with a low SO_4^{2-} content in seawater. In the Permian, marine brines correspond to the Na-K-Mg-Cl-SO_4 (SO_4-rich) chemical type, but important variation occurs in the relative content of sulfate ions as expressed in Jänecke units in fluid inclusions from the early Permian to Late Triassic (Kovalevych *et al.*, 2002*a*, fig. 9).

The first indication of a sulphate-type brine observed in this study appears in cycle 6, where kieserite and polyhalite precipitated in the central parts of the basin associated with evaporative drawdown. The central part of the basin corresponds to the later time of sedimentation, whereas the more marginal areas of the evaporite formation contain sylvite with few $MgSO_4$ minerals. The mineral paragenesis of the marginal areas is interpreted to be an earlier phase in the basin brine evolution for that cycle. A seawater composition where Mg concentration is nearly equal to that of Ca would precipitate sylvite as the first potash mineral, followed by carnallite (Williams-Stroud, 1994*b*). Carnallite precipitates at the expense of sylvite as it is consumed through back reaction with the brine. The presence of kieserite and polyhalite in this cycle suggests that the sulfate content had increased relative to potash beds lower in the sequence. The measured sulphate content of fluid inclusions in this cycle is high, which is consistent with the appearance of magnesium sulphate minerals in this cycle. The content of the sulphate ion was higher than the equivalent content of Ca^{2+}. Accordingly, it may be assumed that $MgSO_4$ occurred in the marine water, which caused the episodic precipitation of kieserite. The relative content of sulphate ions as expressed in Jänecke units in fluid inclusions in halite of cycle 6 (7.7 – see Table 3) is very similar to the average content in the Asselian of Ukraine (8.5 – Kovalevych *et al.*, 2002*b*) and is considerably smaller than the SO_4 content (in Jänecke units) in modern seawater concentrated to the onset of halite sedimentation.

Seawater is the most logical source of sulfate, considering the Br content in the halite (Raup and Hite, 1996), the palaeogeography (Peterson and Hite, 1969; Williams-Stroud, 1994*a*), and the mineralogical composition of the evaporite series (Raup and Hite, 1996). All these data indicate that salts derive predominantly from marine water. The formation of sylvite-carnallite deposits is related to the influence of $CaCl_2$ brines flowing into the basin, especially in the zone of development of the Uncompahgre Trough, from the underlying sedimentary deposits. A considerable $CaCl_2$ concentration in the buried marine brines during hardening of halite deposits and formation of rock salt is fixed in inclusion brines in diagenetic halite (samples 2 and 3 of cycle 10; Table 4).

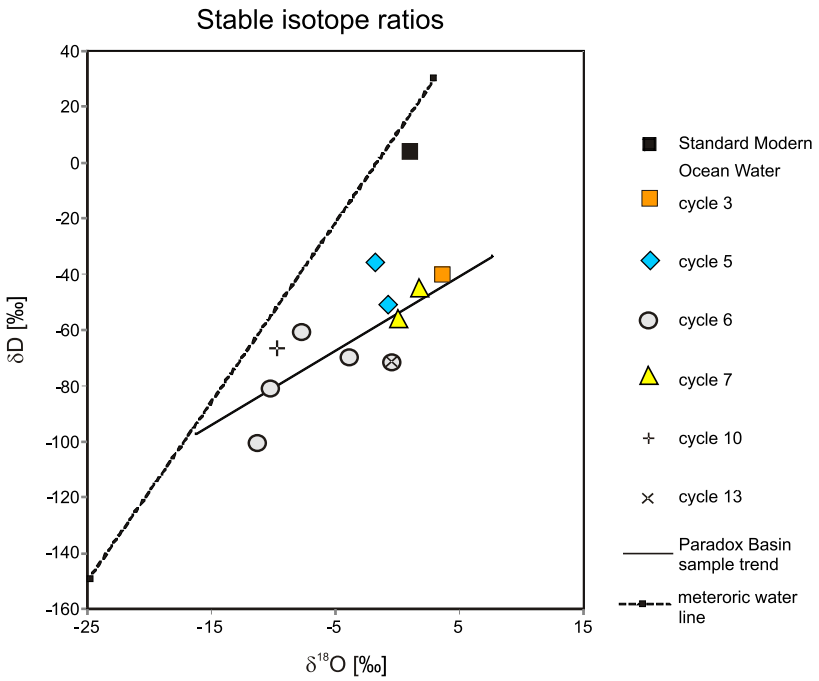

Fig. 5. Stable isotope ratios for fluid inclusions from the Paradox Basin samples

The sample from cycle 10 at 1141 m depth (indicated by the cross symbol) is closest to the meteoric water trend line, supporting a primarily recycled secondary halite origin for that sample

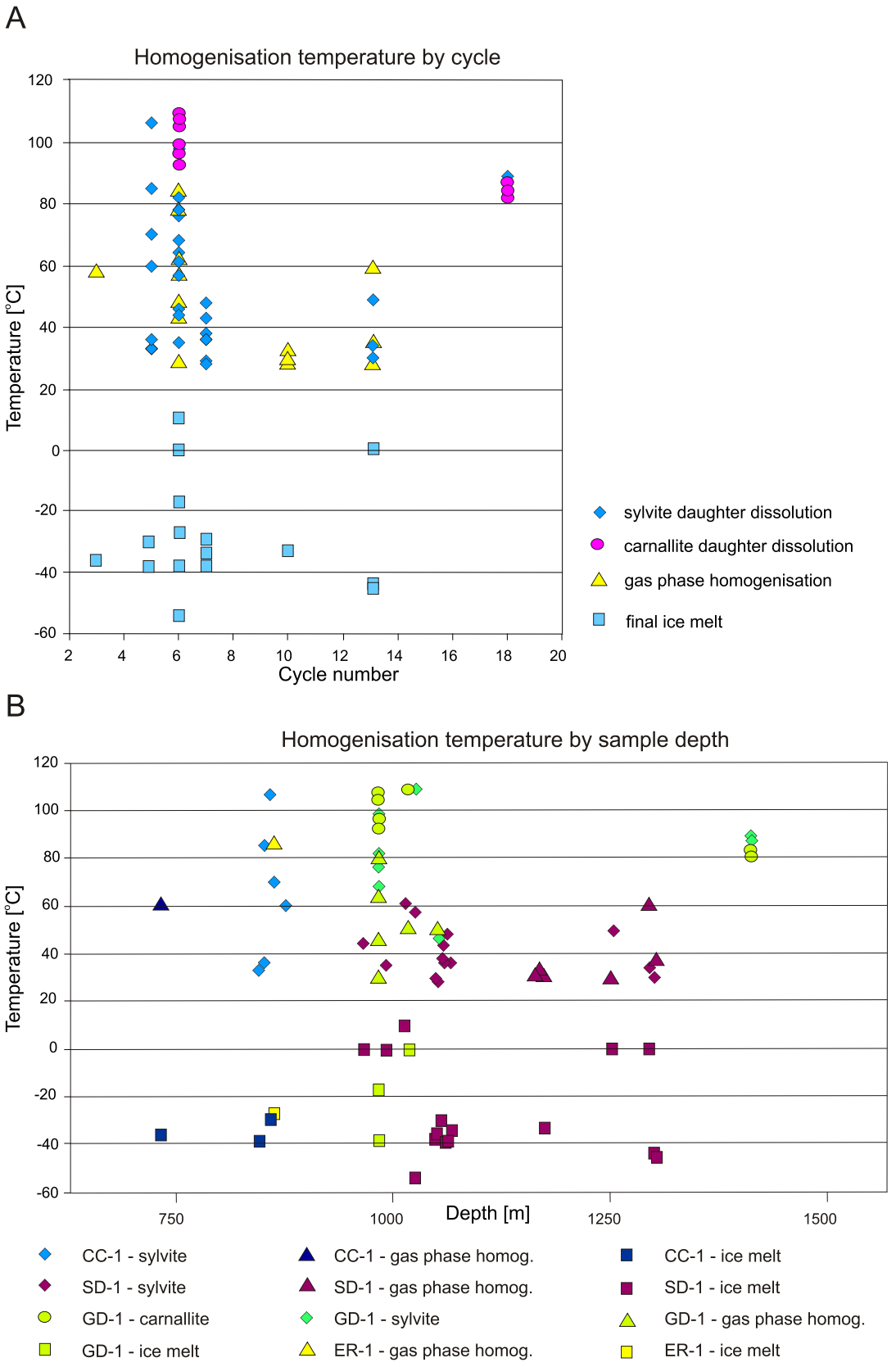

Fig. 6. Homogenisation temperatures of fluid inclusion samples from the different cores

A – chart shows homogenisation temperatures plotted by halite cycle number;
B – chart on the left shows homogenisation temperatures plotted by depth

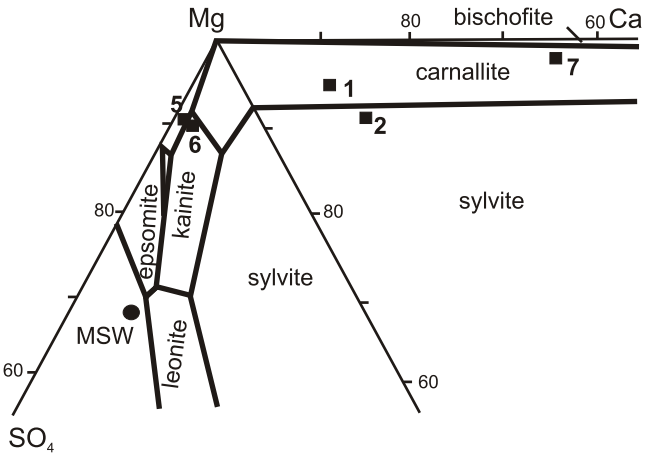

Fig. 7. Average ion contents of the inclusion brines (as shown in Table 3) in primary inclusions of sedimentary halite in sedimentary halite of the Pennsylvanian evaporite formation of the Paradox Basin at a temperature of 25°C plotted on the Jänecke projection of the quinary system Na-K-Mg-SO_4-Cl-H_2O at 25°C

MSW – modern seawater saturated with respect to halite; location of points indicating the composition of brine inclusions in sedimentary halite of the Pennsylvanian evaporite formation of the Paradox Basin at a temperature of 25°C; the black squares with numbers correspond to samples studied

A proposed geochemical model anticipates a steady deficit (with respect to modern marine waters) of the sulphate anion and the steady presence of $CaCl_2$ in basin brines during NaCl precipitation. The erosional contact between the top of each halite bed and the overlying anhydrite indicates a sudden freshening of the basin with dilution of highly-concentrated brines and dissolution of salt. It seems that during the final stages of halite deposition and in some cases of potash deposits, remnant brines were of the chloride type with a considerable $CaCl_2$ concentration. For example, assuming that the interpretation of the zoned inclusions as primary deposition of halite from seawater is correct, this situation is shown by inclusions in the halite of potassium-bearing deposits of cycle 18 (sample 7); it was found that the Ca^{2+} content in those brines could reach 59 g/l (Table 2). Therefore, the inflow of marine waters provided sulphate that caused deposition of the basal bed of calcium sulphate that denotes the next cycle above each halite bed.

Comparing the composition of the deepest halite bed analysed in this study (cycle 18) to the shallowest beds (cycles 3, 5 and 6) the sulphate-poor nature of cycle 18 compared to the high sulphate content of the samples analyse for chemical content in cycle 6 are suggestive of a transition recording a temporal change in seawater composition. Ambiguity exists, however, when the fact that daughter crystals of both sylvite and carnallite are abundant in both the shallow and the deep potash beds. There is no clear correlation between dominance of sylvite over carnallite with depth in the fluid inclusion samples, making the interpretation of the fluid inclusion chemical analyses equivocal. There is no doubt that basin brines were periodically saturated with regard to $CaSO_4$ as indicated by allochthonous anhydrite in fluid inclusions in sedimentary and diagenetic halite in sample 3 from the Shafer Dome 1 core (Fig. 4B) and the consistent presence of anhydrite in rock salt. The anhydrite crystal drapes on top of bottom-growth chevron halite (Raup and Hite, 1992; Williams-Stroud, 1994*a*) are evidence of brine mixing, possibly with meteoric waters that caused precipitation of fine anhydrite crystals into the standing halite-saturated brine. Many of these anhydrite crystals were apparently trapped in large inclusions of the secondary halite.

All of the analytical results (Table 2 and Fig. 7, points 1, 2 and 5–7) are clearly located within and nearby the carnallite field on both 2K-Mg-Ca and 2K-Mg-SO_4 diagrams for 25°C. This very strongly suggest a main marine source of water as waters of other origin do not contain enough Mg^{2+} and K^+ ions. This supports a primary origin of carnallite deposits that is also supported by the presence of authigenic carnallite, which precipitated from relict inclusion brine due to temperature decrease (Fig. 3A, B). As is known (Borchert and Muir, 1964), on the 2K-Mg-SO_4 diagrams for temperatures >40°C the carnallite field decreases considerably in size, and points 5 and 6 are included in the kieserite field that justifies the occurrence of this mineral among sylvite-carnallite deposits (Fig. 7).

The temperature conditions had an essential importance for mineral formation during times of high basin salinity. However, results of homogenisation of inclusions with carnallite or sylvite daughter crystals, which are shown in Table 2 and Figure 6, need comment. There are no special remarks regarding the values of 30–35°C (samples 1, 2 and 4), as those temperatures agree with models for conditions of halite crystallisation in modern, shallow salt lakes with relatively low concentrations of potassium and magnesium salts. Those temperatures, evidently, were typical also of the Paradox Basin at the beginning of halite precipitation.

The values characteristic for the time of precipitation of potassium-magnesium salts (samples 5 and 7) indicate former, high brine temperatures, although it may be supposed that they were lower than the actually measured values (80–100°C). In part, this can be explained by the take off the carnallite or sylvite inclusions during the halite growth (Cendón *et al.*, 1998). This is possible, although it might be expected that such inclusions have various relations between fluid and solid phase and, accordingly, a great scattering of temperature measurements. In the slides studied from samples 5 and 7 the inclusions have the same phase relations and small differences in temperatures with regard to the average value. Therefore, the following explanation is proposed.

Experimentally, it was found that, in well-defined stable conditions, saturated brines become supersaturated with regard to some salts during the temperature decrease (Khamskiy, 1967). Compounds having crystallisation water in their composition are especially susceptible to the formation of supersaturated solutions (Khamskiy, 1967). Carnallite is one such compound. It is possible that during the formation of sedimentary halite in samples 5 and 7 from highly mineralised brines, brines supersaturated with regard to carnallite have been conserved within inclusions. Therefore, the degree of temperature in-

crease regarding real values could depend on the degree of brine supersaturation: the higher the brine supersaturation, the higher the homogenisation values of inclusions. Ignoring this supposition, it is evident that during precipitation of potassium salts the brine temperatures were considerable, although no doubt they were below 100°C. Sample 4 (salt bed 10) is an exception; the halite in this sample originated due to brine mixing (Fig. 4D) at low temperatures (<30°C), as indicated by one-phase fluid inclusions arranged in growth banding in the mineral.

The deuterium and oxygen-18 stable isotope analysis of the fluid inclusions analysed clearly shows the influence of both meteoric water influx and mixing with basin brines (Fig. 5). Both δD and $\delta^{18}O$ are lowered with dilution of seawater with meteoric water. For instance, in the Baltic Sea, which has much lower salinity than seawater due to dilution by meteoric water, values for δD are –50‰ (Friedman *et al*., 1964). The values plotted in Figure 5 and shown in Table 2 are consistent with those measured by Craig (1961) for closed-basin brines relative to the values that define the deuterium and ^{18}O stable isotope ratios for meteoric water. Although the stable isotope analysis clearly supports the meteoric water and basin brine mixing model previously proposed by Williams-Stroud (1994*b*), the geochemical modelling for that study was based on the mineral paragenesis of cycle 5, one of the shallowest halite beds in the Paradox Formation. The analyses presented in this study suggest that the transition from magnesium sulphate-poor to magnesium sulphate-rich (similar to modern seawater) composition occurred prior to deposition of cycle 5. The influence of brine mixing is evident in the halite and potash facies of all salt cycles in the Paradox Formation, but the mineral composition is clearly dominated by solutes supplied to the basin by seawater inflow.

CONCLUSIONS

1. Evidence for the transition of seawater brines of the Na-K-Mg-Ca-Cl characteristic of the Devonian and the lower Carboniferous to the Na-K-Mg-SO_4-Cl seawater brines characteristic of the Permian has been found in the Paradox Evaporite Basin.

2. It appears that between cycles 18 (older) and 10 (younger), the magnesium concentration of the waters in the basin increased so that the lowermost cycles studied contain sylvite without carnallite, then carnallite + sylvite, followed by the magnesium sulphate minerals kieserite and polyhalite. The seawater composition indicated in the younger cycles is still not clearly that of aragonite seas, because sylvite is found in conjunction with magnesium sulphate minerals instead of carnallite. This relationship may be explained by non-equilibrium precipitation of sylvite through cooling of surface brines that are in equilibrium with carnallite (Lowenstein and Spencer, 1990).

3. It is clear that the mineral assemblage of the Paradox Formation represents an intermediate Mg/Ca brine composition between modern seawater and $MgSO_4$-poor seawater, but it is not possible to pinpoint in which cycle (or cycles) the transition occurs. It is more likely that the composition oscillated between the two compositional end-members while a general trend toward $MgSO_4$-rich brines developed. The time required for the switch to aragonite seas could have lasted the entire Desmoinesian – the period spanned by the Paradox Formation.

4. While the stable isotope analyses do not support conclusive interpretation of seawater as the main basin fluid, they are in the range of values supporting a closed basin environment (Craig, 1961) which is consistent with evaporite deposition. The impact of brine mixing is indicated by the isotopes, but the overall mineral paragenesis supports a predominantly marine origin.

Without additional detailed and systematic study of the geochemistry of the halite beds with particular attention to the older potash beds, the possibility that a change in Paradox Basin brine chemistry due to a temporal change in seawater chemistry cannot be unequivocally eliminated. Specifically, resolving ambiguity around the primary *versus* secondary nature of halite fluid inclusions in this deposit could provide a better understanding of the rates of processes affecting seawater composition. The identification of those rates will, in turn, help to better understand the relative importance of the various factors related to changes in the rate of ocean crust production (Hardie, 1996), atmospheric composition, biosphere evolution, and climate change.

Acknowledgements. This paper is devoted to the memory of Dr. A. Kasprzyk. The study resulted from research grant No. 6 P04D 039 16 from the KBN (to V. Kovalevych) and project No. UKRAINA/193/2006 of the Ministry of Science and Higher Education. Chemical analyses were done by the Central Chemical Laboratory, Polish Geological Institute – National Research Institute, and fluid inclusion analyses were done at the Institute of Geology and Geochemistry, National Academy of Sciences of Ukraine. Significant portions of the work were supported by the Maria Skłodowska-Curie Fund II (U.S.G.S./PGI joint project). The authors would like to thank R. Hite for his many helpful discussions about the geochemistry and sedimentology of the Paradox Basin Evaporites, and D. A. Budd, G. Czapowski, J. Horita, V. Kovalevych and T. W. Lyons for their comments on the first version of the paper.

REFERENCES

BORCHERT H. and MUIR R. O. (1964) – Salt deposits: the origin, metamorphism and deformation of evaporites. Van Nostrand.

CENDÓN D. I., AYORA C. and PUEYO J. J. (1998) – The origin of barren bodies in the Subiza potash deposit, Navarra, Spain: implications for sylvite formation. J. Sediment. Res., **68**: 43–52.

CRAIG H. (1961) – Isotopic variations in natural waters. Science, **133**: 1702–1703.

D'ANS J. (1915) – Untersuchungen über die Saltzsysteme ozeanischer Salzablagerungen. Kali, **9**: 48.

DAVIS D. W., LOWENSTEIN T. K. and SPENCER R. J. (1990) – Melting behavior of fluid inclusions in laboratory-grown halite crystals in the systems NaCl-H_2O, NaCl-KCl-H_2O, NaCl-$MgCl_2$-H_2O and NaCl-$CaCl_2$-H_2O. Geochim. Cosmochim. Acta, **54**: 591–601.

FANLO I. and AYORA C. (1998) – The evolution of the Lorraine evaporite basin. Implications for the chemical and isotope composition of the Triassic ocean. Chem. Geol., **146**: 135–154.

FRIEDMAN I., REDFIELD A. C., SCHOEN B. and HARRIS J. (1964) – The variation of the deuterium content of natural waters in the hydrologic cycle. Rev. Geoph., **2**: 177–224.

GALAMAY A. R., BUKOWSKI K. and PRZYBYŁO J. (1997) – Chemical composition and origin of brines in the Badenian evaporite basin of the Carpathian Foredeep: fluid inclusion data from Wieliczka (Poland). Slovak Geol. Mag., **3**: 165–171.

GARCÍA-VEIGAS J., ROSELL L. and GARLICKI A. (1997) – Petrology and geochemistry (fluid inclusions) of Miocene halite rock salts (Badenian, Poland). Slovak Geol. Mag., **3**: 181–186.

GOLDHAMMER R. K., OSWALD E. J. and DUNN P. A. (1994) – High-frequency, glacio-eustatic cyclicity in the Middle Pennsylvanian of the Paradox Basin: an evaluation of Milankovitch forcing. IAS Spec. Publ., **19**: 243–283.

HARDIE L. A. (1984) – Evaporites, marine or non-marine? Am. J. Sc., **284**: 193–240.

HARDIE L. A. (1996) – Secular variation in seawater chemistry: an explanation for the coupled secular variation in the mineralogies of marine limestones and potash evaporites over the past 600 m.y. Geology, **24**: 279–283.

HARDIE L. A., SMOOT J. P. and EUGSTER H. P. (1981) – Saline lakes and their deposits: a sedimentological approach. IAS Spec. Publ., **2**: 7–41.

HITE R. J. (1961) – Potash-bearing evaporite cycles in the salt anticlines of the Paradox Basin, Colorado and Utah. U.S. Geol. Surv., Prof. Paper, **424-D**: 135–138.

HITE R. J. (1970) – Shelf carbonate sedimentation controlled by salinity in the Paradox Basin, southeast Utah. In: Third International Symposium on Salt. Northern Ohio Geol. Soc., Cleveland: 48–66.

HITE R. J. (1983) – The sulfate problem in marine evaporites. Sixth International Symposium on Salt, **I**: 217–230. The Salt Inst.

HITE R. J. (1985) – Preliminary mineralogical and geochemical data from the D.O.E. Gibson Dome corehole no. 1, San Juan County, Utah. U.S. Geol. Surv. Open-File Report, **83–780**.

HITE R. J. and BUCKNER D. H. (1981) – Stratigrahic correlations, facies concepts, and cyclicity in Pennsylvanian rocks of the Paradox Basin. In: Rocky Mountain Association of Geologists, 1981 Field Conference (techn. coord. D. L. Wiegland): 147–159.

HOLLAND H. D. (1984) – The chemical evolution of the atmosphere and oceans. Princeton University Press, Princeton, New Jork.

HORITA J., ZIMMERMANN H. and HOLLAND H. D. (2002) – Chemical evolution of seawater during the Phanerozoic: implications from the record of marine evaporites. Geochim. Cosmochem. Acta, **66**: 3733–3756.

JOHNSON S. Y., CHAN M. A. and KONOPKA E. A. (1991) – Pennsylvanian and Early Permian paleogeography of the Uinta-Piceance Basin Region, northwest Colorado and Northeast Utah. U.S. Geol. Surv. Bull., **1787-CC**: 1–35.

KENDALL A. C. (1988) – Aspects of evaporite basin stratigraphy. In: Evaporites and Hydrocarbons (ed. B. C. Schreiber): 11–65. Columbia University Press, New York.

KENDALL A. C. (2011) – Marine evaporites. Geol. Ass. Canada, GeoText, **6**: 503–537.

KHAMSKIY E. V. (1967) – Kristallizatsiya iz rastvorov. Nauka, Leningrad.

KOVALEVICH V. M. (1988) – Phanerozoic evolution of ocean water composition. Geochem. Intern., **25**: 20–27.

KOVALEVYCH V. and VOVNYUK S. (2010) – Fluid inclusions in halite from marine salt deposits: are they real micro-droplets of ancient seawater? Geol. Quart., **54** (4): 401–412.

KOVALEVICH V. M., PERYT T. M. and PETRICHENKO O. I. (1998) – Secular variation in seawater chemistry during the Phanerozoic as indicated by brine inclusions in halite. J. Geol., **106**: 695–712.

KOVALEVYCH V., PERYT T. M., BEER W., GELUK M. and HALAS S. (2002*a*) – Geochemistry of Early Triassic seawater as indicated by study of the Roet halite in the Netherlands, Germany and Poland. Chem. Geol., **182**: 549–563.

KOVALEVYCH V. M., PERYT T. M., CARMONA V., SYDOR D. V., VOVNYUK S. V. and HALAS S. (2002*b*) – Evolution of Permian seawater: evidence from fluid inclusions in halite. Neues Jahrb. Geol. Paläont. Abh., **178** (1): 27–62.

KYSER T. K. (1987) – Equilibrium fractionation factors for stable isotopes. Miner. Ass. Canada, **13**: 1–84.

LAZAR B. and HOLLAND H. (1988) – The analysis of fluid inclusions in halite. Geochim. Cosmochim. Acta, **52**: 485–490.

LOWENSTEIN T. K. (1982) – Primary features in a potash evaporite deposit, the Permian Salado Formation of west Texas and New Mexico. SEPM Core Workshop, **3**: 276–304.

LOWENSTEIN T. K. and SPENCER R. J. (1990) – Syndepositional origin of potash evaporites: petrographic and fluid inclusion evidence. Am. J. Sc., **290**: 1–42.

LOWENSTEIN T. K., TIMOFEEFF M. N., BRENNAN S. T., HARDIE L. A. and DEMICCO R. V. (2001) – Oscillations in Phanerozoic seawater chemistry: evidence from fluid inclusions. Science, **294**: 1086–1088.

PETERSON J. A. and HITE R. J. (1969) – Pennsylvanian evaporite-carbonate cycles and their relation to petroleum occurrence, Southern Rocky Mountains. Am. Ass. Petrol. Geol. Bull., **53**: 884–908.

PETRICHENKO O. I. (1979) – Methods of study of inclusions on minerals of saline deposits. In: Fluid Inclusion Research Proc. COFFI (ed. E. Roedder), **12**: 214–274. University of Michigan Press, Ann Arbor.

PETRICHENKO O. I. and WILLIAMS-STROUD S. (1995) – Chemical composition of water in the Late Carboniferous Evaporite Paradox Basin (USA). In: Abstracts, 13th Intern. Congress on Carboniferous-Permian, Polish Geological Institute: 160–161.

PETRYCHENKO O. Y. (1973) – Metody doslidzhennya vkluchen u mineralakh galogennykh porid. Naukova Dumka, Kyiv.

PETRYCHENKO O. Y. and PERYT T. M. (2004) – Geochemical conditions of deposition in the Upper Devonian Prypiac' and Dnipro-Donets evaporite basins (Belarus and Ukraine). J. Geol., **112**: 577–592.

PETRYCHENKO O. Y., PERYT T. M. and CHECHEL E. I. (2005) – Early Cambrian seawater chemistry from fluid inclusion in halite from Siberian evaporites. Chem. Geol., **219**: 149–161.

PETRYCHENKO O., PERYT T. M. and ROULSTON B. (2002) – Seawater composition during deposition of Viséan evaporites in the Moncton Subbasin of New Brunswick as inferred from the fluid inclusion study of halite. Canadian J. Earth Sc., **39**: 157–167.

RAUP O. B. (1970) – Brine mixing: an additional mechanism for formation of basin evaporites. Am. Ass. Petrol. Geol. Bull., **54**: 2246–2259.

RAUP O. B. and HITE R. J. (1992) – Lithology of evaporite cycles and cycle boundaries in the upper part of the Paradox Formation of the Hermosa Group of Pennsylvanian Age in the Paradox Basin, Utah and Colorado. U.S. Geol. Surv. Bull., **2000-O**: 1–47.

RAUP O. B. and HITE R. J. (1996) – Bromine geochemistry of chloride rocks of the Middle Pennsylvanian Paradox Formation of the Hermosa Group, Paradox Basin, Utah and Colorado. U.S. Geol. Surv. Bull., **2000-M**: 1–116.

ROEDDER E. (1984) – Fluid inclusions. Rev. Miner., **12**.

SPENCER R. J. and HARDIE L. A. (1990) – Control of seawater composition by mixing of river waters and mid-ocean ridge hydrothermal brines. Geochem. Soc. Spec. Publ., **2**: 409–419.

TRUDGILL B. D. (2011) – Evolution of salt structures in the northern Paradox Basin: controls on evaporite deposition, salt wall growth and supra-salt stratigraphic architecture basin research. Basin Res., **23**: 208–238.

VALIASHKO M. G. (1962) – Zakonomernosti formirovaniya mestorozhdeniy soley. Izd. Moscow University, Moskva.

WEBER L. J., SARG J. F. and WRIGHT F. M. (1995) – Sequence stratigraphy and reservoir delineation of the Middle Pennsylvanian (Desmoinesian), Paradox Basin and Aneth Field, southwestern USA. SEPM Short Course Notes, **35**: 1–81.

WENGERD S. A. (1958) – Pennsylvanian stratigraphy, Southwest Shelf, Paradox Basin. In: Guidebook to the Geology of the Paradox Basin (ed. A. F. Sanbom): 109–134. 9th Ann. Field Conf. Intermountain Ass. Petrol. Geol.

WILLIAMS-STROUD S. (1994*a*) – The evolution of inland sea of marine origin at a non-marine saline lake: the Pennsylvanian Paradox Salt. SEPM Spec. Publ., **50**: 293–306.

WILLIAMS-STROUD S. (1994*b*) – Solution to the Paradox? results of some chemical equilibrium and mass balance calculations applied to the Paradox Basin evaporite deposit. Am. J. Sc., **294**: 1189–1228.

ZHARKOV M. A. (1984) – Paleozoic Salt Bearing Formations of the World. Springer, Berlin.

ZIMMERMANN H. (2000) – Tertiary seawater chemistry – implications from primary fluid inclusions in marine halite. Am. J. Sc., **300**: 723–767.